

A search for time-integrated CP violation in $D^0 \rightarrow h^- h^+$ decays

M. J. Charles^{1,a}, on behalf of the LHCb collaboration.

Department of Physics, University of Oxford, Oxford, United Kingdom

Abstract. The preliminary results of a search for time-integrated CP violation in $D^0 \rightarrow h^- h^+$ ($h = K, \pi$) decays performed with 0.6 fb^{-1} of data collected by LHCb in 2011 are presented. The flavour of the charm meson is determined by the charge of the slow pion in the $D^{*+} \rightarrow D^0 \pi^+$ and $D^{*-} \rightarrow \bar{D}^0 \pi^-$ decay chains. The difference in CP asymmetry between $D^0 \rightarrow K^- K^+$ and $D^0 \rightarrow \pi^- \pi^+$, $\Delta A_{CP} \equiv A_{CP}(K^- K^+) - A_{CP}(\pi^- \pi^+)$, is measured to be $\Delta A_{CP} = [-0.82 \pm 0.21(\text{stat.}) \pm 0.11(\text{syst.})] \%$. This differs from the hypothesis of CP conservation by 3.5σ .

1 Introduction

The time-integrated CP asymmetry, $A_{CP}(f)$, for the final states $f = K^- K^+$ and $f = \pi^- \pi^+$ has two contributions: an indirect component (to a good approximation universal for CP eigenstates in the Standard Model) and a direct component (in general final state dependent). In the limit of U-spin symmetry, the direct component is equal and opposite in sign for $K^- K^+$ and $\pi^- \pi^+$ [1]. In the Standard Model, CP violation is expected to be small [2,3,1]. However, in the presence of physics beyond the Standard Model the rate of CP violation could be enhanced [1,4]. No prior evidence of CP violation in the charm sector has been found.

The most precise measurements to date of the time-integrated CP asymmetries in $D^0 \rightarrow K^- K^+$ and $D^0 \rightarrow \pi^- \pi^+$ were made by the CDF, BABAR, and BELLE collaborations [5,6,7]. LHCb has previously reported preliminary results based on 37 pb^{-1} of data collected in 2010 [8]. In the limit that the efficiency for selected events is independent of the decay time, the difference between the two time-integrated asymmetries, $\Delta A_{CP} \equiv A_{CP}(K^- K^+) - A_{CP}(\pi^- \pi^+)$, is equal to the difference in the direct CP asymmetry. However, if the dependence of the efficiency on the decay time is different for the $K^- K^+$ and $\pi^- \pi^+$ final states, a contribution from indirect CP violation remains. The Heavy Flavor Averaging Group (HFAG) has combined time-integrated and time-dependent measurements of CP asymmetries taking account of the different decay time acceptance to obtain world-average values for the indirect CP asymmetry of $a_{CP}^{\text{ind}} = (-0.03 \pm 0.23)\%$ and the difference in direct CP asymmetry between the final states of $\Delta a_{CP}^{\text{dir}} = (-0.42 \pm 0.27)\%$ [9].

In these proceedings, LHCb results [10,11] for the measurement of the difference in integrated CP asymmetries between $D^0 \rightarrow K^- K^+$ and $D^0 \rightarrow \pi^- \pi^+$, performed with approximately 0.6 fb^{-1} of data collected in 2011, are presented. The initial state (D^0 or \bar{D}^0) is tagged by requiring a $D^{*+} \rightarrow D^0 \pi^+$ decay. The use of charge-conjugate modes is implied throughout, except in the definition of asymmetries.

2 Formalism

The raw asymmetry for tagged D^0 decays to a final state f is given by $A_{\text{raw}}(f)$, defined as:

$$A_{\text{raw}}(f) \equiv \frac{N(D^{*+} \rightarrow D^0(f)\pi^+) - N(D^{*-} \rightarrow \bar{D}^0(\bar{f})\pi^-)}{N(D^{*+} \rightarrow D^0(f)\pi^+) + N(D^{*-} \rightarrow \bar{D}^0(\bar{f})\pi^-)}, \quad (1)$$

where $N(X)$ refers to the number of reconstructed events of decay X after background subtraction.

The raw asymmetries may be written as a sum of various components, coming from both physics and detector effects:

$$A_{\text{raw}}(f) = A_{CP}(f) + A_D(f) + A_D(\pi_s) + A_P(D^{*+}). \quad (2)$$

Here, $A_{CP}(f)$ is the intrinsic physics CP asymmetry, $A_D(f)$ is the asymmetry for selecting the D^0 decay into the final state f , $A_D(\pi_s)$ is the asymmetry for selecting the ‘slow pion’ from the D^{*+} decay chain, and $A_P(D^{*+})$ is the production asymmetry for prompt D^{*+} mesons. The asymmetries A_{CP} , A_D and A_P are defined in the same fashion as A_{raw} .

For a two-body decay of a spin-0 particle to a self-conjugate final state there can be no D^0 detection asymmetry, i.e. $A_D(K^- K^+) = A_D(\pi^- \pi^+) = 0$. Moreover, to first order $A_D(\pi_s)$ and $A_P(D^{*+})$ cancel out in the difference

$$A_{\text{raw}}(K^- K^+) - A_{\text{raw}}(\pi^- \pi^+),$$

leaving a quantity, defined as ΔA_{CP} , equal to the difference in physics asymmetries:

$$\Delta A_{CP} \equiv A_{CP}(K^- K^+) - A_{CP}(\pi^- \pi^+), \quad (3)$$

$$= A_{\text{raw}}(K^- K^+) - A_{\text{raw}}(\pi^- \pi^+). \quad (4)$$

To minimize second order effects, related to the slightly different kinematic properties of the two decay modes, the analysis is done in bins of the relevant kinematic variables, as shown later in Secs. 4 and 5. The physics asymmetry of each final state may be written at first order as [12]:

$$A_{CP}(f) \approx a_{CP}^{\text{dir}}(f) + \frac{\langle t \rangle}{\tau} a_{CP}^{\text{ind}}, \quad (5)$$

^a e-mail: m.charles1@physics.ox.ac.uk

where $a_{CP}^{\text{dir}}(f)$ is the asymmetry coming from direct CP violation for the decay, $\langle t \rangle$ is the average decay time in the sample used, τ the true D^0 lifetime, and a_{CP}^{ind} is the asymmetry associated with CP violation in the mixing. To a good approximation this latter quantity is universal [1], and so

$$\Delta A_{CP} = \left[a_{CP}^{\text{dir}}(K^- K^+) - a_{CP}^{\text{dir}}(\pi^- \pi^+) \right] + \frac{\Delta \langle t \rangle}{\tau} a_{CP}^{\text{ind}}, \quad (6)$$

where $\Delta \langle t \rangle$ is the difference in average decay time of the D^0 mesons in the $K^- K^+$ and $\pi^- \pi^+$ samples. In the limit that $\Delta \langle t \rangle$ vanishes, ΔA_{CP} probes the difference in direct CP violation between the two decays.

3 Dataset and selection

A description of the LHCb detector may be found in Ref. [13]. The field direction in the LHCb dipole is such that charged particles are deflected in the horizontal plane. The current direction in the dipole was changed several times during data taking; about 60% of the data was taken with one polarity and 40% with the other.

Selections are applied to provide samples of $D^{*+} \rightarrow D^0 \pi^+$ candidate decays, with $D^0 \rightarrow K^- K^+$ and $\pi^- \pi^+$. A loose D^0 selection including a mass window of full width 100 MeV/c^2 was already applied during data taking, in the final stage of the high level trigger (HLT). In the offline analysis only candidates that were accepted by this trigger algorithm are considered. Both the offline and HLT selections impose a variety of requirements on kinematics and decay time to isolate the decays of interest, including requirements on the track fit quality, on the D^0 and D^{*+} vertex fit quality, on the transverse momentum of the D^0 ($p_T > 2 \text{ GeV}/c$), on the decay time t of the D^0 ($ct > 100 \mu\text{m}$), on the helicity angle of the D^0 decay, that the D^0 points back to a primary vertex, and that the D^0 daughter tracks do not. Fiducial requirements are imposed to ensure that the tagging soft pion lies within the central region of the detector acceptance. In addition, the offline analysis exploits the capabilities of the RICH system to distinguish between pions and kaons when reconstructing the D^0 .

Defining the mass difference as $\delta m \equiv m(h^+ h^- \pi^+) - m(h^+ h^-) - m(\pi^+)$, the mass and mass difference spectra of selected candidates are shown in Figs. 1 and 2, respectively. The difference in width between the $K^- K^+$ and $\pi^- \pi^+$ mass spectra arises from the different opening angles of the two decays. The D^{*+} signal yields are approximately 1.44×10^6 in the tagged $K^- K^+$ sample, and 0.38×10^6 in the tagged $\pi^- \pi^+$ sample. The fractional difference in average decay time of D^0 candidates passing the selection between the $K^- K^+$ and $\pi^- \pi^+$ samples is $\Delta \langle t \rangle / \tau = (9.8 \pm 0.9)\%$.

4 Fit procedure

Fits are performed on the samples in order to determine $A_{\text{raw}}(K^- K^+)$ and $A_{\text{raw}}(\pi^- \pi^+)$. The analysis is performed in 54 kinematic bins, divided by p_T and pseudorapidity (η) of the D^{*+} candidates, momentum of the tagging soft pion, and whether the initial trajectory of the slow pion is towards the left or right half of the detector. A binning is imposed for the reason that the production and detection

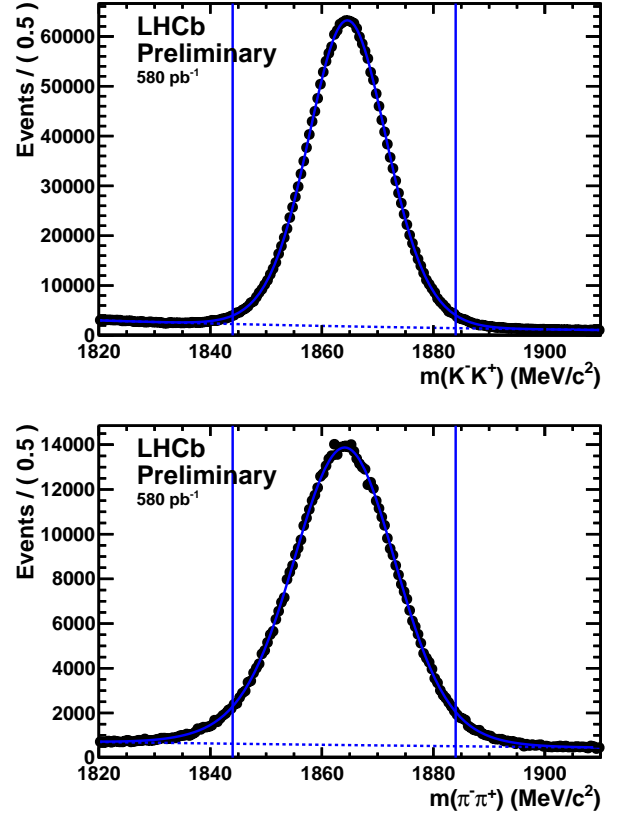


Fig. 1. Fits to the $m(K^- K^+)$ and $m(\pi^- \pi^+)$ spectra of D^{*+} candidates passing the selection and satisfying $0 < \delta m < 15 \text{ MeV}/c^2$. The vertical blue lines indicate the signal window of 1844–1884 MeV/c^2 .

asymmetries can in general vary with p_T and η , and so can the detection efficiency of the two different D^0 decays, in particular through the effects of the particle identification requirements.

The events are further partitioned in two ways. First, the data are divided between the two dipole magnet settings. Second, the first 350 pb^{-1} of data are processed separately from the remainder, with the division aligned with a break in data taking due to a LHC technical stop. In total, therefore, 216 independent measurements are considered for each decay mode.

One-dimensional fits to the mass difference spectra are performed. The fits include separate components for the signal and background lineshapes. The signal is described as the sum of two Gaussian functions with a common mean, convolved with an asymmetric function. The background is described by an empirical function of the form

$$\left[1 - e^{-(\delta m - \delta m_0)/c} \right],$$

where δm_0 and c are parameters describing the threshold and shape of the function, respectively. In each case an unbinned maximum likelihood fit is used. The D^{*+} and D^{*-} samples are fitted simultaneously and share several shape parameters, though a charge-dependent offset in the central value and overall scale factor in the mass resolution are allowed. The raw asymmetry in the yields of the signal component is extracted directly from this simultaneous

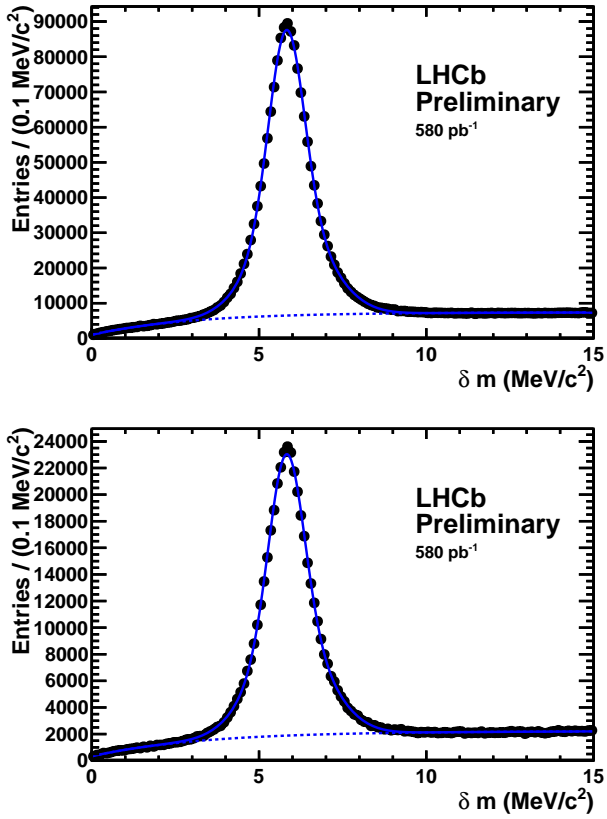


Fig. 2. Fits to the mass difference spectra, where the D^0 is reconstructed in the final states $K^- K^+$ (top) and $\pi^- \pi^+$ (bottom), with a D^0 mass lying in the window of 1844–1884 MeV/c^2 .

fit. An example fit from one measurement bin is shown in Fig. 3.

The one-dimensional fits used for the tagged data do not distinguish between correctly reconstructed signal and backgrounds that peak in the mass difference. Such backgrounds can arise from D^{*+} decays in which the correct slow pion is found but the D^0 is partially mis-reconstructed. However, these backgrounds are suppressed by the use of tight particle identification requirements and a narrow D^0 mass window. From studies of the D^0 mass sidebands this contamination is found to be approximately 1% of the signal yield.

5 Results and systematic uncertainties

A value of ΔA_{CP} is determined in each measurement bin using the results for $A_{\text{raw}}(K^- K^+)$ and $A_{\text{raw}}(\pi^- \pi^+)$. The χ^2/ndf of these measurements has a value of 211/215. A weighted average is performed to yield the result $\Delta A_{CP} = (-0.82 \pm 0.21)\%$.

Numerous robustness checks are made, including monitoring the value of ΔA_{CP} as a function of time (Fig. 4), re-performing the measurement with more restrictive RICH particle identification requirements, and using a different D^{*+} selection. Potential biases due to the inclusive hardware trigger selection are investigated with the subsample of data in which one of the signal final-state tracks is directly responsible for the hardware trigger decision. In all cases good stability is observed.

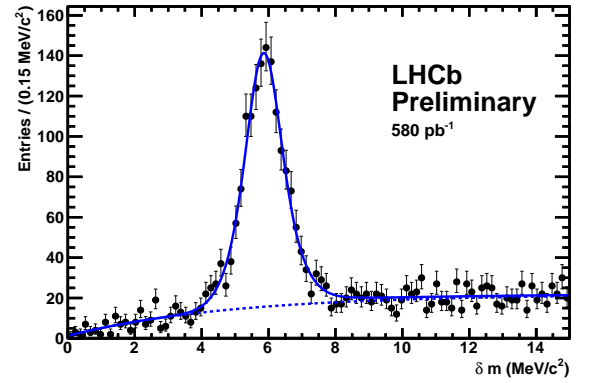


Fig. 3. Example fit used in the ΔA_{CP} analysis. The first kinematic bin of the first run period with magnet up polarity is shown for the $D^0 \rightarrow K^- K^+$ final state.

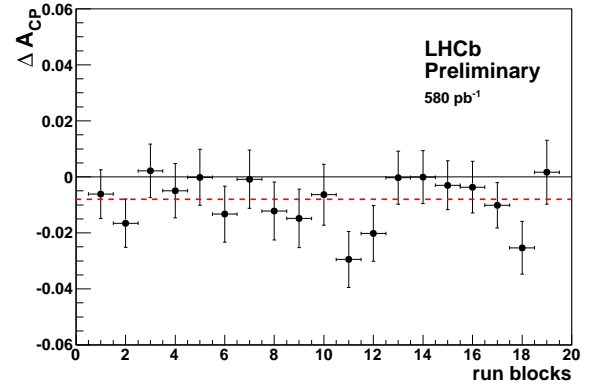


Fig. 4. Time-dependence of the measurement. The data are divided into 19 disjoint, contiguous, time-ordered blocks and the value of ΔA_{CP} measured in each block. The red dashed line shows the result for the combined sample.

Table 1. Summary of absolute systematic uncertainties for ΔA_{CP} .

Effect	Uncertainty
Fiducial requirement	0.01%
Peaking background asymmetry	0.04%
Fit procedure	0.08%
Multiple candidates	0.06%
Kinematic binning	0.02%
Total	0.11%

Systematic uncertainties are assigned by loosening the fiducial requirement on the soft pion; by assessing the effect of potential effect peaking background in toy Monte Carlo studies; by repeating the analysis with the asymmetry extracted through sideband subtraction instead of a fit; with all candidates but one (chosen at random) removed in events with multiple candidates; and comparing with the result obtained with no kinematic binning. In each case the full value of the change in result is taken as the systematic uncertainty. These uncertainties are listed in Table 1. The sum in quadrature is 0.11%.

6 Conclusions

LHCb has measured the time-integrated difference in CP asymmetry between $D^0 \rightarrow K^- K^+$ and $D^0 \rightarrow \pi^- \pi^+$ decays, $\Delta A_{CP} = (a_{CP}^{\text{dir}}(K^- K^+) - a_{CP}^{\text{dir}}(\pi^- \pi^+)) + 0.098 a_{CP}^{\text{ind}}$, to be

$$\Delta A_{CP} = [-0.82 \pm 0.21(\text{stat.}) \pm 0.11(\text{syst.})] \%$$

with 0.6 fb^{-1} of 2011 data, where the first uncertainty is statistical and the second systematic. Combining the statistical and systematic uncertainties in quadrature, the significance of the measured deviation from zero is 3.5σ . The result is consistent with the current HFAG world average [9].

Subsequent to this result being presented, several papers on the theoretical interpretation have been written, examining the possible size and uncertainty in the SM contribution and considering possible new physics contributions. A partial list may be found in Ref. [14,15,16,17,18,19,20,21,22]. We thank our theory colleagues for their help in understanding this result.

Acknowledgements

We express our gratitude to our colleagues in the CERN accelerator departments for the excellent performance of the LHC. We thank the technical and administrative staff at CERN and at the LHCb institutes, and acknowledge support from the National Agencies: CAPES, CNPq, FAPERJ and FINEP (Brazil); CERN; NSFC (China); CNRS/IN2P3 (France); BMBF, DFG, HGF and MPG (Germany); SFI (Ireland); INFN (Italy); FOM and NWO (The Netherlands); SCSR (Poland); ANCS (Romania); MinES of Russia and Rosatom (Russia); MICINN, XuntaGal and GENCAT (Spain); SNSF and SER (Switzerland); NAS Ukraine (Ukraine); STFC (United Kingdom); NSF (USA). We also acknowledge the support received from the ERC under FP7 and the Region Auvergne.

References

1. Y. Grossman, A. L. Kagan and Y. Nir, Phys. Rev. D **75** (2007) 036008.
2. S. Bianco, F. L. Fabbri, D. Benson and I. Bigi, Riv. Nuovo Cim. **26N7** (2003) 1.
3. M. Bobrowski, A. Lenz, J. Riedl and J. Rohrwild, JHEP **1003** (2010) 009.
4. I. I. Bigi, M. Blanke, A. J. Buras and S. Recksiegel, JHEP **0907** (2009) 097.
5. CDF Collaboration, T. Aaltonen *et al.*, arXiv:1111.5023 [hep-ex] (submitted to Phys. Rev. D)
6. BABAR Collaboration, B. Aubert *et al.*, Phys. Rev. Lett. **100** (2008) 061803.
7. Belle Collaboration, M. Staric *et al.*, Phys. Lett. B **670** (2008) 190.
8. LHCb Collaboration, LHCb-CONF-2011-023.
9. Heavy Flavor Averaging Group, D. Asner *et al.*, arXiv:1010.1589 [hep-ex]; http://www.slac.stanford.edu/xorg/hfag/charm/EPS11/DCPV/direct_indirect_cpv.html.
10. LHCb Collaboration, LHCb-CONF-2011-061.
11. LHCb Collaboration, R. Aaij *et al.*, arXiv:1112.0938 [hep-ex] (submitted to Phys. Rev. Lett.).
12. I. I. Bigi, A. Paul and S. Recksiegel, JHEP **1106** (2011) 089.
13. LHCb Collaboration, A. A. Alves *et al.*, JINST **3** (2008) S08005.
14. G. Isidori, J. F. Kamenik, Z. Ligeti and G. Perez, arXiv:1111.4987 [hep-ph].
15. J. Brod, A. L. Kagan and J. Zupan, arXiv:1111.5000 [hep-ph].
16. K. Wang and G. Zhu, arXiv:1111.5196 [hep-ph].
17. A. N. Rozanov and M. I. Vysotsky, arXiv:1111.6949 [hep-ph].
18. D. Pirtskhalava and P. Uttayarat, arXiv:1112.5451 [hep-ph].
19. Y. Hochberg and Y. Nir, arXiv:1112.5268 [hep-ph].
20. H.-Y. Cheng and C.-W. Chiang, arXiv:1201.0785 [hep-ph].
21. B. Bhattacharya, M. Gronau and J. L. Rosner, arXiv:1201.2351 [hep-ph].
22. X. Chang, M.-K. Du, C. Liu, J.-S. Lu and S. Yang, arXiv:1201.2565 [hep-ph].